THE BELL SYSTEM TECHNICAL JOURNAL
Vol. 56, No. 4, April 1977
Printed in U.S.A.

Pseudorandom Noise Loading for Noise Power Ratio and Law of Addition

By R. H. MOSELEY, S. B. PIRKAU, and R. B. SWERDLOW

(Manuscript received July 29, 1976)

A noise-loading measurement set is described, which uses coherent averaging to measure intermodulation noise that lies below thermal noise. This technique also lends itself to a new way of measuring the addition of intermodulation noise over a string of repeaters. Noise loading and law of addition data are presented.

I. INTRODUCTION

Noise loading has been used for many years to test wideband communications systems.[1] In this technique, the system load is simulated by thermal noise of the same bandwidth and total power as the actual load. This is particularly effective for equipment designed to carry hundreds of telephone circuits, because the multiplexing together of many independent circuits naturally leads to a total signal that is gaussian. Small frequency bands (notches), usually a few kilohertz wide, are eliminated from the thermal noise load at several places in the band. This noise signal is applied to the device under test, and the noise that appears at the notch frequencies after the device is detected and measured. The noise in these narrow notches is a fairly accurate measure of the circuit noise that a customer would overhear. This noise may be broken down into several components: thermal, intermodulation, interference, and so on. In modern, long-haul, repeatered telephone systems, intermodulation noise is usually a big contributor that must be held at or below the thermal noise, which limits the power at which each repeater may be operated. Until now, intermodulation noise was usually measured by raising the output power until intermodulation became far larger than the thermal noise. This is possible since intermodulation noise increases with an increase of input power and thermal noise does not. The difficulty with this approach is that the noise is then being measured outside of the equipment-design range. Another important factor in estimating the total intermodulation noise for many tandem

repeaters is that, since intermodulation depends on the input signal, there is the possibility of coherent addition of this noise between repeaters. The degree of coherency, or law of addition, has been estimated in the past by connecting several repeaters in tandem and measuring the intermodulation noise of the string. Since many repeaters (about 12 or more) are needed to estimate the addition accurately, this is difficult to do in the laboratory.

In 1971, work was started on a new noise-loading scheme to measure intermodulation noise that is below thermal noise and to estimate the law of addition. The scheme replaces the thermal-noise source by one that is periodic but appears to be noise-like: a pseudorandom noise source. The intermodulation noise is produced from the signal through the nonlinearity of the repeater. It has the same basic period as the input signal and so may be coherently detected and summed at the device output. As successive periods are summed, the intermodulation noise will add on a voltage basis, but the thermal noise will add on a power basis. Thus, a 3-dB enhancement is achieved with each doubling of the number of periods of the source.

A test set to perform this measurement was completed in 1973. The basic layout, special features, and test results of the instrument are described in Section II. Estimation of intermodulation noise for many repeaters in tandem, using the pseudorandom noise loading (PRNL) test set, is described in Section III, and test results are presented. The chief advantages of this test set are summarized in the conclusions, Section IV.

II. OVERVIEW OF OPERATION

The pseudorandom noise loading (PRNL) test set is comprised of three main units: a transmitter section to generate the broadband noise source, a receiver section that includes an analog-to-digital converter and memory for coherent addition of the measured signal, and a master timing unit to achieve repetitive and coherent operation of the transmitter and receiver sections. The noise signal may be applied to the test device at either baseband, IF or RF (4 GHz).

The power in the notch is preselected at the output of the device being tested by the PRNL receiver. The receiver has a noise figure of 10 dB or better at IF and 8 dB at baseband. Due to these low noise figures, the noise floor below which signal averaging is required is usually set by the noise figure of the test device. Up to 42-dB improvement in signal to noise is possible by the averaging process, corresponding to the summation of 16,384 successive periods of the pseudorandom test signal. Ninety seconds of averaging is required to achieve the 42-dB improvement.

The ultimate capability is determined by noise in the notch that is

Table I — Attainable notch depth

Baseband	Signal Power (dBm)	Notch Depth (dB)	Notch Frequencies (MHz)
380 kHz to 20 MHz IF	0	80	3.886, 11.7, 17.842
60 to 80 MHz RF	2	96	63.886, 71.7, 77.842
Any 20-MHz channel in the 3.7- to 4.2-GHz band	6	35	No notch filters at RF: notches at baseband and IF are translated to the RF channel

coherent with the signal. This is due to leakage of signal through the notch filter and intermodulation from the transmitter at higher output power. These limits are given in Table I.

The notch depth is enhanced when the test device has gain. The gain allows source levels to be low, which, in turn, reduces intermodulation from active devices in the source. A notch depth limit of 120 dB due to filter characteristics can be realized at IF and RF with sufficient gain.

2.1 PRNL transmitter

Shown in Fig. 1 is a block diagram of the PRNL transmitter. The noise source is a 25-stage shift register operating at 300 MHz. The output is a very long pseudorandom digital sequence at the bit rate of 300 Mb/s. The digital signal is first band limited from 380 kHz to 20 MHz by bandpass filter BP1 to form a noise source having statistics close enough to gaussian to approximate the telephone load. Reference 2 gives the

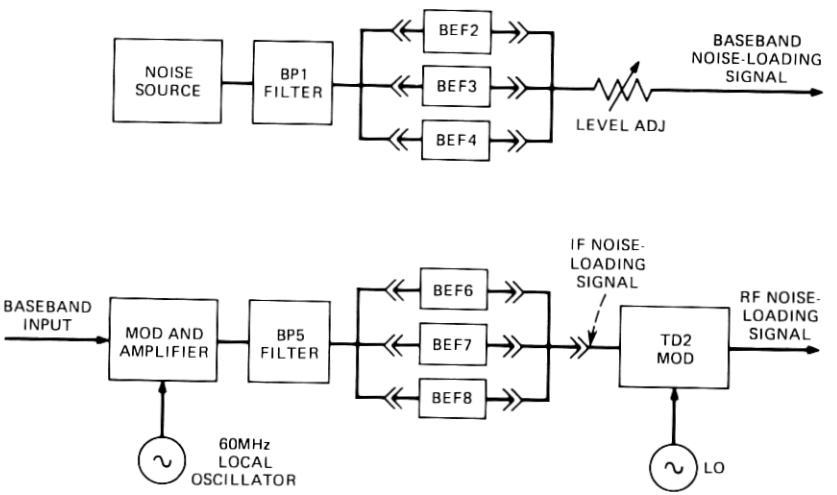

Fig. 1—PRNL transmitter.

statistics of the signal for various filter bandwidths. As a comparison, separate noise-loading curves were run on the same amplifier, using thermal and pseudorandom noise sources. Within the range where the intermodulation noise was sufficiently above thermal noise level, the two results agreed to 0.1 dB, which is within the measurement accuracy of the test.

Next, one of three band-elimination filters (BEF2, BEF3, and BEF4) is selected. These filters are narrow band-stop filters with an 80-dB rejection band, 6 kHz wide, centered at 3.886, 11.7, and 17.842 MHz, respectively. The signal is next level adjusted at baseband. Lowering the signal level before all the active devices in the signal path assures lowest intermodulation from the test set and, consequently, the deepest notches. This signal may be used to load at baseband. To load at IF, the signal is then up converted to an IF center frequency of 70 MHz by a modulator and 60-MHz local oscillator (LO).

The IF signal is first amplified and then passed through BPF5. This filter passes the upper sideband while attenuating the lower sideband by 60 dB and the LO signal by 90 dB. At this point in the transmitter, the notch depth (for a broadband power of 0 dBm) has been reduced to 50 dB due to intermodulation in the modulator.

To obtain a notch depth of 120 dB (at $f_c \pm 2$ kHz, where f_c is the notch-center frequency), the proper IF band-stop filter (BEF6, 7, or 8) is selected to align in frequency with the translated baseband notch. The IF notch frequencies are 63.886, 71.7, and 77.842 MHz. As shown in Fig. 1, this signal is applied to the device under test for IF noise loading. When an RF (4-GHz) noise-loading signal is required, an up converter and the associated tuners and filters are used to translate the noise load to RF. Notch depths at RF are limited to 46 dB by the up converter for broadband power levels of 0 dBm.

2.2 PRNL receiver

A block diagram of the receiver is shown in Fig. 2. For detection of a 4-GHz signal, RF preselection provides a 1-MHz signal centered on the notch frequency. This signal is then attenuated and down converted to IF. Attenuation is necessary to insure that the intermodulation products produced in the down converter are at least 20 dB lower than the signal to be measured. To insure coherency, the same LO source used to up convert to RF must be used to down convert to IF.

The first function performed at IF is that of preselection by narrowband (±1.5-kHz) crystal filters. Since the signal being preselected may be 80 dB lower than the loading signal, multistage preselection and amplification is used. The multistage process produces a gain of 75 dB and out-of-band rejection of 120 dB. The noise figure of the IF receiver

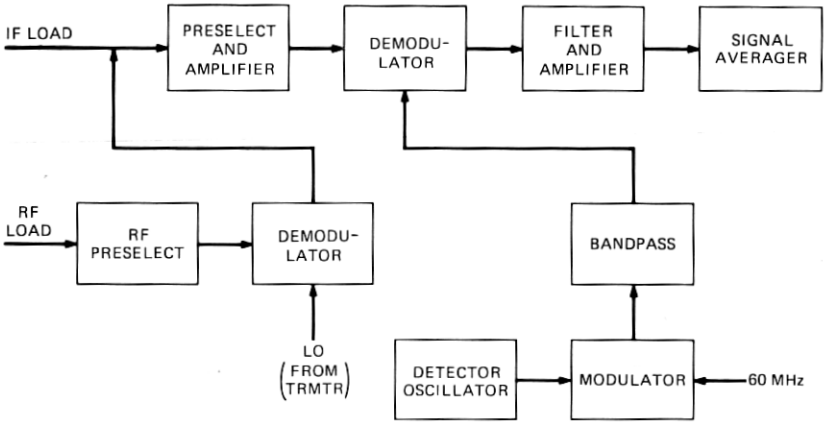

Fig. 2—PRNL receiver.

is determined by the preselect filter which varies between 5.4 and 8 dB of loss, depending on the frequency of preselection. The preselected signal is then down converted to baseband in a single stage of demodulation. The LO for this stage of demodulation is generated by mixing the IF transmitter LO (60 MHz) and the detector oscillator (set to 6 kHz below the baseband notch frequency) and selecting the sum frequency. The resulting notch signal is centered at 6 kHz, whereupon it is filtered and detected.

2.3 Final detection

The final detection process is performed by the signal-averaging unit. This is a commercial unit slightly modified to meet the specific requirements of PRNL. The functions performed by the averager are analog-to-digital conversion, storage, summation of the digitized signal, and the ability to play back the stored signal in real time for measurement with a power meter. The analog-to-digital converter takes a 9-bit sample of the input signal every 20 μs and stores it in an 18-bit register. Since there are 1024 word locations in the register, a repetitive signal with a period of 20 ms could be handled. In practice, a period of 5.28 ms is used and 256 samples taken during each period. The number, N, of successive sweeps by the averager is preselected for values of M ($2^M = N$) up to 14. The coherency of the detection process is preserved by starting successive averager sweeps at the start time of the pseudorandom source and at a fixed phase of the detection oscillator. This timing is performed by the master timing circuit described in Section 2.4.1. The digitized sample points are summed to corresponding locations in memory for each sweep.

Finally, the stored word in the averager can be played back in real time.

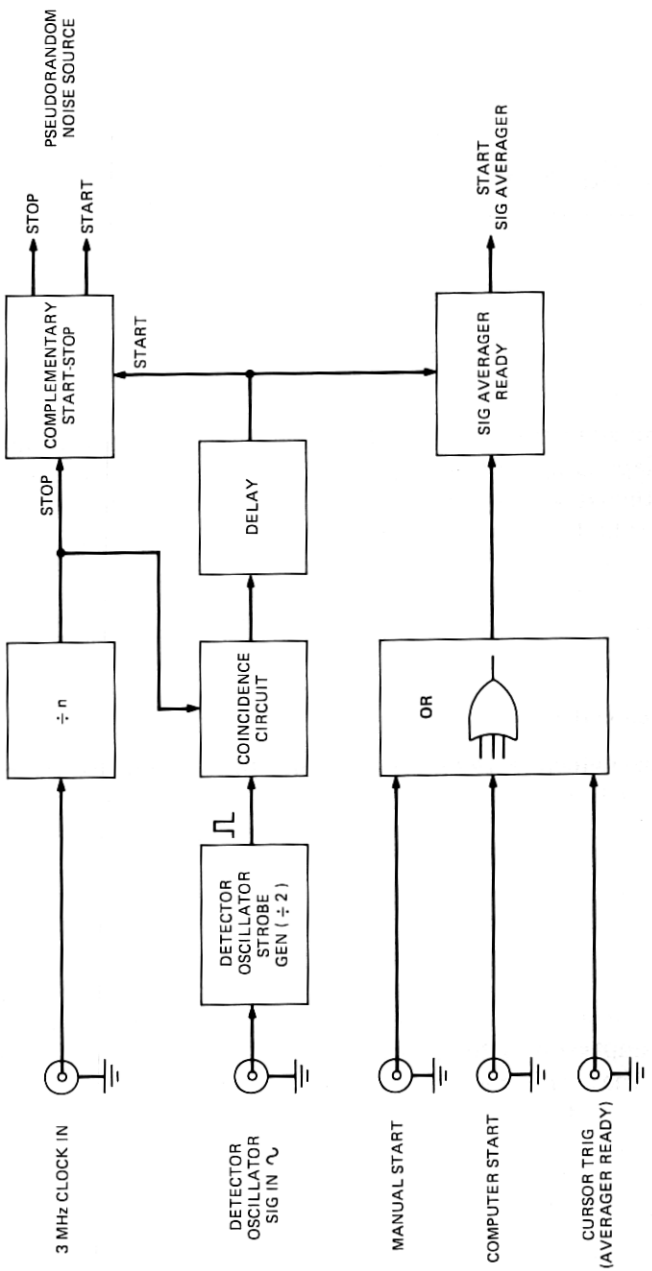

Fig. 3—Master timing circuit.

The real-time play-back signal can be displayed on an oscilloscope, applied to a spectrum analyzer, or to a power meter. The signal averager is also interfaced with a computer. The computer can be used to control the measurement and to further process the data. The computer interface is described in Section 2.4.2.

2.4 Special features

2.4.1 Master timing circuit

The heart of the noise loading set is the master timing circuit. The three major functions of the circuit are to

(*i*) Lock the start of the pseudorandom data transmitter and signal averager to a common oscillator (detector oscillator), which demodulates the signal in the notch to baseband.

(*ii*) Start the signal averager.

(*iii*) Start-stop the pseudorandom data transmitter.

Of the three functions listed above, synchronization (lock) is most important since it is essential for coherent signal addition. A simplified block diagram of the master timing circuit is shown in Fig. 3.

The critical section of this circuit is the coincidence function. The coincidence circuit phase-locks the relative high-frequency notch-detector strobe pulse (3.6 to 17.8 MHz) to the low-frequency divide-by-*n* counter output pulse (approximately 200 Hz). The resulting output pulse is used to initiate functions (*ii*) and (*iii*) above, thus insuring coherent operation of the PRNL set.

A second PRNL set, with 6-GHz capabilities, is under construction. This set is discussed in more detail in Appendix C. The major difference (besides the 6-GHz capability) is the absence of the above described coincidence circuit. In the new PRNL set, the LO as well as all notch-detect LOs are derived from one master oscillator, thereby assuring a constant phase relationship between all LO signals. The disadvantage of this design is, of course, less flexibility due to fixed notch-detect LO frequencies.

2.4.2 Computer interface

Another one of the features of the PRNL set is its operating capability through computer control, which permits unattended operation and data processing for law of addition measurements. The setup is illustrated in Fig. 4.

The program that operated the noise-loading set could operate either through a teletype request or automatically. In either mode, the computer sends a start command to the PRNL set. The PRNL set synchronizes this computer start command with its internal start commands and

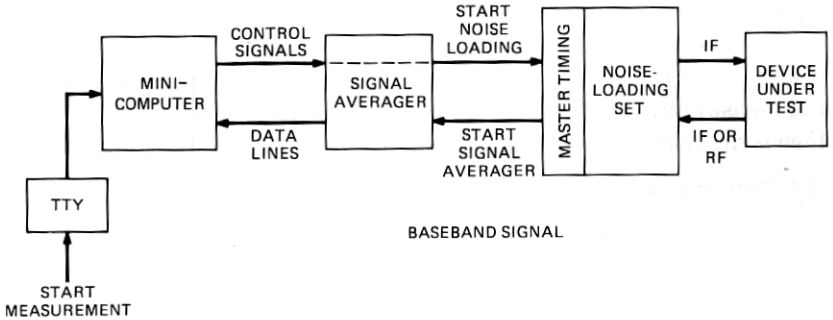

Fig. 4—Computer-controlled noise-loading data collection.

executes a measurement. Upon completion of the measurement, the PRNL set sends a finish command to the computer which, in turn, initiates a data transfer from the memory of the signal averager to the computer disk memory for storage. The automatic mode of operation was used to make repetitive measurements through the use of the real-time clock of the computer. In this mode, a measurement can be requested, either at a specified time, or at a specific interval.

2.5 Calibration

The purpose of calibrating the noise-loading test set is to obtain an absolute measure of the intermodulation signal in a notch at the output of the device under test and to establish the signal power density near the notch frequency. The difference in these measurements yields the noise-power ratio (NPR) which is a measure of the linearity of the device.

The precise calibration relates the power as measured at the signal-averager output for one cycle of the averager to the power in the notch at the output of the test device. To do this, the receiver was calibrated to determine the equivalent noise bandwidth of each set of preselect filters, and the gain of the receiver was measured for the center frequency of each set of preselection filters.

The intermodulation signal in the notch at the output of the device under test is determined by level adjusting the power as measured at the signal-averager output by the measured receiver gain and the amount of averaging performed. The signal-power density near the notch frequency is found by measuring the total output power at the output of the test device and subtracting the selectivity of the receiver.

2.6 NPR results

Two important features of the PRNL test set are the averaging feature and the multifrequency capability. Both are important for characterizing intermodulation noise in a repeater. The averaging feature permits NPR

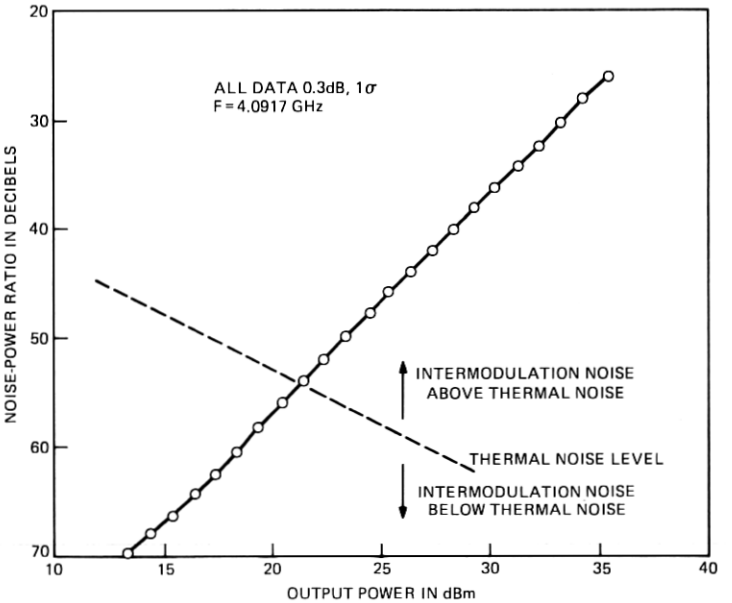

Fig. 5—Noise loading results for a 4-GHz TWT.

measurements below thermal noise. The multifrequency feature allows measurements on portions of the repeater so that the effect of these parts can be seen on the overall NPR performance. The data shown below illustrate both these points.

Examples of data showing the averaging and multifrequency capabilities of the set are shown in Figs. 5 and 6. In Fig. 5, the device under

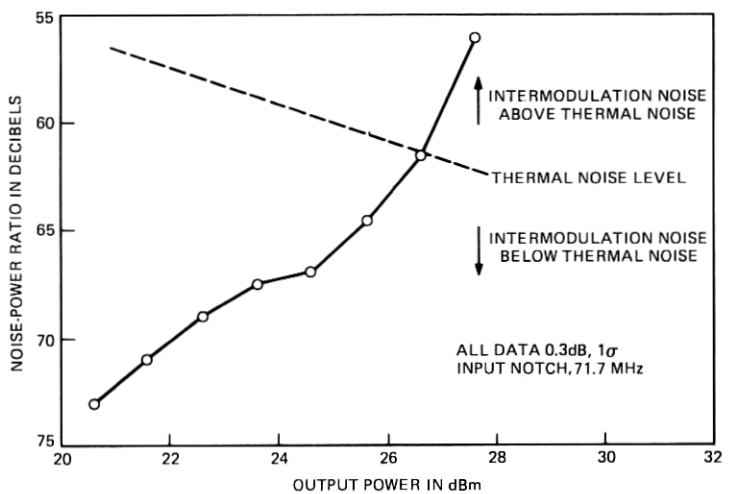

Fig. 6—Noise loading results for an SSB radio transmitter (70-MHz input, 4-GHz output).

test was a 4-GHz traveling-wave tube (TWT) measured RF-to-RF. The figure shows the measured NPR (ordinate) as a function of the TWT output power (abscissa). At an output power of 21.4 dBm, the thermal-noise power in the notch equalled the intermodulation (IM) power in the notch. The test set residual IM was 50 dB lower due to the high TWT gain. The 2:1 slope indicates dominance of third-order intermodulation products. Multifrequency capability of the PRNL set is illustrated in Fig. 6. Shown are the results of an IF-to-RF noise-loading measurement on an experimental single-sideband transmitter that includes a TWT. In this measurement, the thermal and intermodulation powers in the notch are equal for an output power of 28.5 dBm. The NPR performance of the additional units (besides the TWT) that make up a transmitter account for the noticeable change in the results shown in Figs. 5 and 6.

III. TANDEM PERFORMANCE AND THE LAW OF ADDITION

Telephone transmission over more than a few miles requires repeaters to maintain adequate speech volume. Since intermodulation is produced by the signal at each repeater, intermodulation from tandem repeaters may be coherent and add on a voltage basis. For instance, in a system of 150 repeaters, the difference in output intermodulation power at the end of the string between coherent and random addition is 22 dB. It would be helpful to have a way of quantifying and predicting this addition for a few repeaters in the laboratory, since direct measurement of many tandem repeaters in the laboratory or field can be expensive.

We show below that the intermodulation power at the end of a tandem string is related only to the crosscorrelation of the intermodulation signals from all pairs of repeaters. Therefore, the crosscorrelation can be used as a quantitative measure of the buildup of intermodulation noise. Since the PRNL set can measure the crosscorrelation, when linked to a computer, it is a tool that we can use to predict the addition of intermodulation products for many similar repeaters by measurements on a few repeaters in the field or laboratory. Data are shown to substantiate the relationship between total intermodulation noise power and the crosscorrelation. The theory and results here hold only for linear systems. Digital and band-limiting repeaters using frequency modulation (FM) cannot be handled by these techniques.

3.1 The model for intermodulation addition

Figure 7 is a schematic representation of a model of a repeater used to study intermodulation noise addition for linear repeaters. The assumption is made that the repeater can be split into two parts: a purely linear part (linear filter) followed by a purely nonlinear part (gain). This is not the most general case, but works well for microwave radio re-

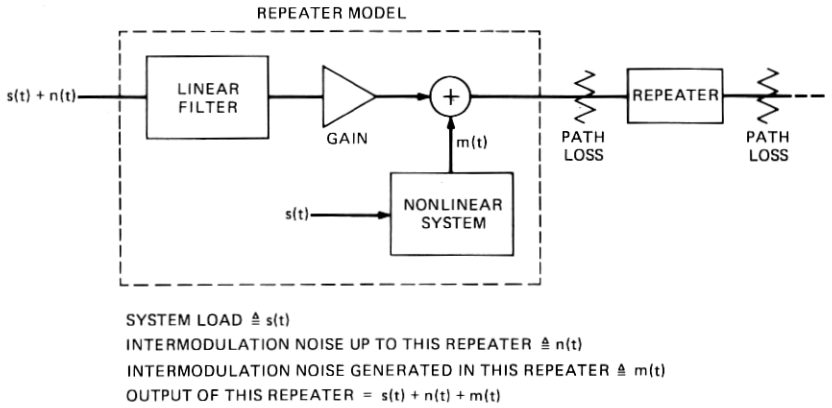

Fig. 7—System model for tandem response.

peaters, where the power stage that generates most of the intermodulation noise is broadband, and for certain cable repeaters.

The critical point of this model is that the intermodulation produced by the repeater, $m(t)$, depends only on the signal, $s(t)$, not the incoming intermodulation, $n(t)$. This is easily demonstrated. Suppose the nonlinear device is third order so that its intermodulation noise increases 3 dB for every dB increase in total power. Since the intermodulation must be small for a practical system, take it to be 40 dB down from the signal. In the next repeater, the signal will produce intermodulation 40 dB down from its level; but the incoming intermodulation will generate intermodulation that is 120 dB down from the signal-induced intermodulation. Such low-level signals will not affect system performance and may be ignored. In other words, the system is purely linear to small signals such as intermodulation. With the assumption that the noise generated at a repeater does not depend on the incoming noise, the total noise at the end of a tandem connection of repeaters is just the sum of these separately produced noise signals. The power of the total noise then depends on the average of products of the noise signals, which are correlations of these signals.

3.2 Experimental validation of model

The point we wish to test is that the total intermodulation from all repeaters in a tandem connection is the sum of the intermodulation from each repeater, where the intermodulation from each repeater is produced independently of the intermodulation from all other repeaters. To demonstrate this, the PRNL set was connected to the input of the first repeater and the output of the last repeater of four experimental single-sideband repeaters that were connected in tandem. The NPR of this arrangement was measured as a function of power, with all repeaters at

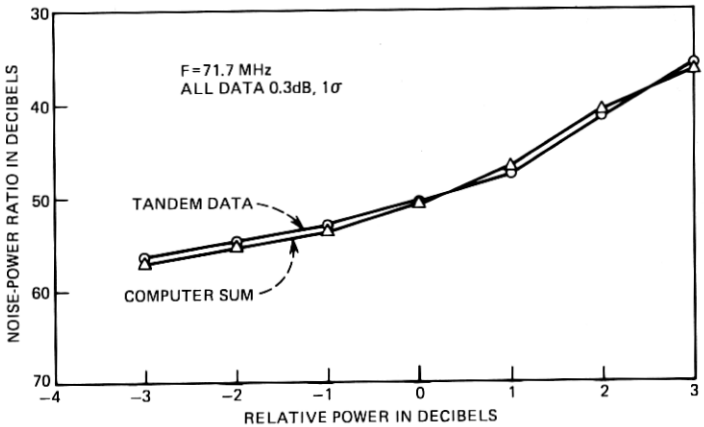

Fig. 8—Noise-loading tandem measurement.

nominal operating conditions. This result is plotted in Fig. 8 as the tandem data curve. Next, the first repeater was kept at nominal load, but the gain controls in the remaining three repeaters were adjusted to keep the transmitters, which generate most of the intermodulation, at low power. In this way, the intermodulation at the end had to be only that from the first repeater.* Notice that the intermodulation traversed all three remaining repeaters, just as when all repeaters were at nominal power. This is important when the repeaters are frequency selective, with even small amounts of delay distortion across the band, since the intermodulation from each repeater passes through different numbers of repeaters and so is distorted differently. For many repeaters in tandem, this effect can lead to considerable decorrelation of the products.

Measurement of intermodulation from each repeater proceeded in the same way with the repeater to be measured at nominal power and all others at low power. The PRNL set recorded the voltage waveform of the intermodulation from each measurement and transferred the resultant digital representation to a computer, as described in Section 2.4.2. These voltage waveforms were added together in the computer the power was computed for the composite waveform, and the results plotted in Fig. 8 labeled computer sum. The two curves are well within measurement accuracy, which substantiates the claim of addition of intermodulation.

The intermodulation is normally below the thermal noise, but in this experiment, it was at least 20 dB under the excess thermal noise created when repeaters were operated at low gain. The experiment could not have been performed without the noise-reduction capability of the PRNL set.

* This technique was proposed by H. Miedema of Bell Laboratories.

3.3 Tandem performance in terms of correlations

In Appendix A, formulas are derived for the intermodulation noise power over a string of repeaters in terms of the correlations between the noise from pairs of repeaters. The correlations available from the noise-loading set are calculated as

$$M_{ij}(0) = \int_{-T/2}^{T/2} v_i(t)v_j(t)dt, \tag{1}$$

where T is the period of the pseudorandom source, and $v_i(t)$, $v_j(t)$ are the intermodulation-noise voltages measured at the input of the PRNL set. This quantity was calculated using a computer interface with the set, as described in Section 2.4.2. As pointed out in Appendix A, eq. (10), $M_{ij}(0)$ is a sample of the broadband intermodulation-noise spectrum, $\mu_{ij}(\omega)$. The particular frequency sampled depends on $G(\omega)$, the preselect filter transfer function.

The intermodulation noise in terms of these correlations is given by eq. (7), repeated here:

$$p_n = \int_{-T/2}^{T/2} v^2(t)dt = \sum_{i=1}^{N} M_{ii}(0) + \sum_{i=1}^{N-1} \sum_{j=i+1}^{N} M_{ij}(0), \tag{2}$$

where p_n is the intermodulation-noise power at the end of N repeaters in tandem and $v(t)$ the intermodulation-noise voltage. The correlation is defined as

$$\rho = \frac{M_{ij}(0)}{\sqrt{M_{ii}(0)M_{jj}(0)}} \tag{3}$$

and is a function of frequency, since $M_{ij}(0)$ is a function of frequency.

If ρ is a constant for a particular type of repeater, then eq. (2) may be used to extrapolate results on just a few repeaters, for which ρ has been measured, to N in tandem. Other formulae are given in Appendix A, where the effects of the linear portions of the repeaters may be studied. $M_{ij}(0)$ includes the effects of the linear filter part of the repeater, as well as the nonlinear part, as expressed in eq. (12) in Appendix A:

$$\mu_{ij}(\omega) = \psi_{ij}\hat{H}_i(\omega)\hat{H}_j^*(\omega). \tag{4}$$

$\hat{H}_i(\omega)$ is the overall linear transfer function from the output of the ith repeater to the Nth repeater, as illustrated in Fig. 9. According to our model, ψ_{ij}, the correlation between the intermodulation noise from the nonlinear element of repeater i to that of repeater j, is independent of frequency.

3.4 Experimental results

Correlations were calculated for the four experimental repeaters mentioned in Section 3.2 using the correlation technique described of

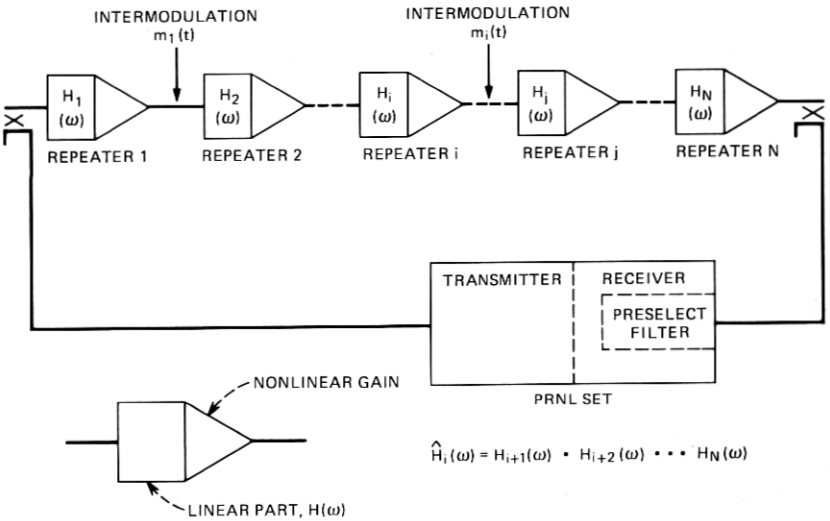

Fig. 9—Intermodulation measurement for tandem repeaters.

reducing the power on all repeaters but the one of interest in order to isolate the intermodulation noise from that repeater. The total noise of all four in tandem was also measured. Results of the correlations for various power settings at the 71.7-MHz notch are given in Fig. 10; the tandem results are shown in Fig. 11.

In Fig. 10, the circles give the mean correlation of the measurements, and the error bars indicate one standard deviation from the mean as

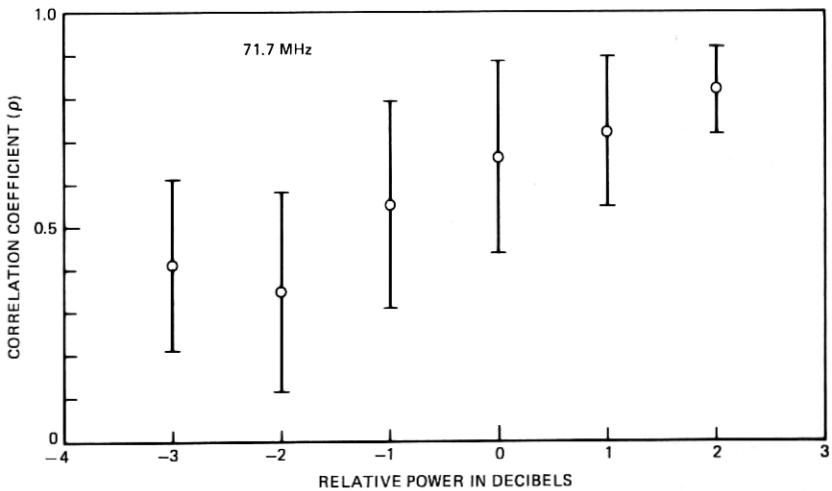

Fig. 10—Intermodulation correlation vs power at 71.7 MHz.

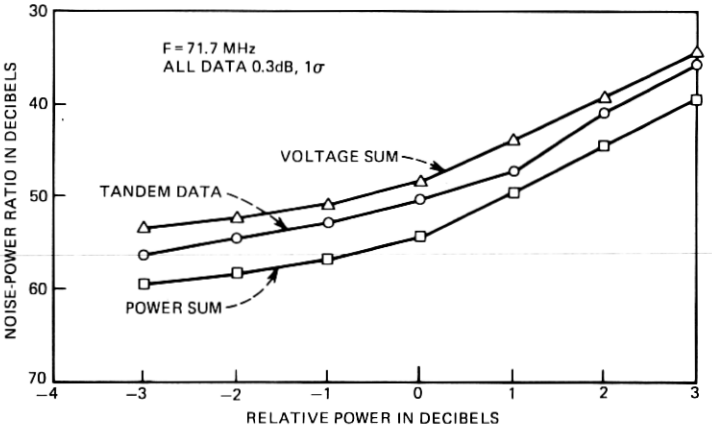

Fig. 11—Noise-loading tandem measurement.

computed from the data. The error in a correlation measurement is reviewed in Appendix B and shown to be about 10 percent. Thus, the large deviations observed must be attributed to the variability in intermodulation correlation between the repeaters. Although the data shown are all positive, negative correlations are possible and were observed.

The curve labeled "tandem data" in Fig. 11 is the actual total NPR measured for the four repeaters in tandem at power levels corresponding to those in Fig. 10. For comparison, results assuming power ($\rho = 0$) or voltage ($\rho = 1$) addition are included by appropriately summing the NPRs from each repeater at a given power level.

A rough comparison of the results of Figs. 10 and 11 can be made by referring to eq. (18) in Appendix A. This indicates, with some manipulation, that the tandem-data curve should have an NPR less than that for the power-sum curve by $10 \log[1 + (N - 1)\rho] = 10 \log(1 + 3\rho)$. For example, at a relative power of −2 dB, the spread in correlation implies an NPR worse than power addition by 1.1 to 4.5 dB; for +1 dB relative power, the spread is 4.2 to 5.7 dB. The maximum is 6 dB for $\rho = 1$, or voltage addition. The broad range in correlation of Fig. 10 therefore corresponds to a broad range in the possible tandem-data curves of Fig. 11, of which the curve shown is just one possibility. The filter characteristics of these repeaters were fairly flat at the midband of 70 MHz, so the range of values of Fig. 10 were probably due to variability in the intermodulation noise produced by the nonlinear elements.

We can see from Fig. 10 that power addition does not occur anywhere in the measured power range for this type of repeater, despite the clear dissimilarity between repeaters. This means that, for a large number of repeaters, intermodulation addition will approach a voltage law, as predicted by eq. (19) in Appendix A.

IV. CONCLUSIONS

The pseudorandom noise-loading set has made accurate, reliable, reproducible noise-loading measurements of intermodulation noise that is below thermal noise. This has permitted testing single-sideband repeaters in their nominal operating power range, tests that would not have been possible using conventional noise loading. The set has multifrequency capability that allows testing of pieces of a heterodyne system as well as the whole. Another unique capability of the set, when linked to a computer, is the computation of correlation of intermodulation noise between different repeaters. Estimates of the addition of intermodulation products on a tandem connection of repeaters can be made from these correlations.

APPENDIX A

Tandem Response Using Correlation

The tandem response of a single-sideband system can be calculated, using the repeater model shown in Fig. 9. The basic assumption of this model, as explained in the text, is that the intermodulation is produced by the signal load and not by other intermodulation signals. Three calculations are made in this appendix. First, the intermodulation power as measured by a noise loading set on a tandem connection of repeaters is shown to depend only on the crosscorrelation of intermodulation noise on pairs of repeaters. Crosscorrelation can be computed from the digital output of the PRNL set. Secondly, the crosscorrelations are broken down to show explicitly the relationship between the crosscorrelation of intermodulation noise and the linear filter part of each repeater. These two results on correlations permit prediction of the addition of intermodulation for many repeaters from measurements on a few. Lastly, the relationship between correlations and a quantity, known as the law of addition, are given. This quantity is often used as a figure of merit for a tandem connection of repeaters.

A.1 Intermodulation in terms of correlations

For this calculation, refer to Fig. 9. The PRNL set is being used to measure N repeaters in tandem, with each repeater modelled as in Fig. 7. The preselect filter on the noise-loading set has been brought out separately; its transfer function is $H(\omega)$, and its impulse response is $h(t)$. Now suppose that the intermodulation time function recorded at the PRNL set from the ith repeater is $v_i(t)$, and from the jth, $v_j(t)$. These functions might be measured using the technique explained in Section 3.2 of the text. The crosscorrelation of these two functions for zero shift can be found as[4]

$$M_{ij}(0) = \int_{-T/2}^{T/2} v_i(t)v_j(t)dt, \tag{5}$$

where T is the period of the PRNL source. This number may be calculated as a sum, using the digital representation of $v(t)$. Since the total intermodulation noise is

$$v(t) = \sum_{i=1}^{N} v_i(t), \tag{6}$$

the power is

$$p_n = \int_{-T/2}^{T/2} v^2(t)dt = \sum_{i=1}^{N} M_{ii}(0) + 2\sum_{i=1}^{N-1}\sum_{j=i+1}^{N} M_{ij}(0), \tag{7}$$

which is the desired result. In Sections A.1 through A.3, the units are volts, kilohms, and milliwatts. All voltages are normalized by dividing them by the square root of the effective input resistance of the PRNL set.

A.2 Effect of linear filters on the correlation

Consider the effect of the preselect filter of the PRNL set on an intermodulation measurement. Call the broadband intermodulation noise from each repeater, as seen at the final repeater, $q_i(t)$ for the ith repeater. If $g(t)$ is the impulse response of the preselect filter, $G(\omega)$ its Fourier transform, then

$$v_i(t) = q_i(t)*g(t), \tag{8}$$

where $v_i(t)$ is the intermodulation measured by the PRNL set, as given in the last section, and the asterisk is convolution. Then, by the techniques of Ref. 4,

$$M_{ij}(\tau) = \int_{-\infty}^{\infty} |G(\omega)|^2 \mu_{ij}(\omega) e^{j\omega\tau} d\omega \tag{9}$$

and

$$M_{ij}(0) = \int_{-\infty}^{\infty} |G(\omega)|^2 \mu_{ij}(\omega) d\omega, \tag{10}$$

where $M_{ij}(t)$ is the crosscorrelation of v_i with v_j, and $\mu_{ij}(\omega)$ is the spectrum of the correlation of the broadband noise, $q_i(t)$ with $q_j(t)$. This says simply that the preselect filter acts as a window on $\mu_{ij}(\omega)$. Usually only $M_{ij}(0)$ is computed, since this is what is needed for the power estimation from eq. (7). The addition of products is a function of ω, and $G(\omega)$ selects the ω of interest. For example, in Fig. 10, the ω is $2\pi \times 71 \times 10^6$ Mrad/s.

Now consider the effect of the linear filters associated with the repeaters. According to Fig. 9, $\hat{H}_i(\omega)$ is the net tandem linear response of the repeaters *after* the ith one until the end of the string. If $m_i(t)$ is the intermodulation noise generated in the ith repeater, then

$$q_i(t) = m_i(t)*\hat{h}_i(t), \tag{11}$$

where $q_i(t)$ is the broadband intermodulation voltage, as defined earlier, and $\hat{h}_i(t)$ is the impulse response, the Fourier transform of $\hat{H}_i(\omega)$. By the arguments of Ref. 4,

$$\mu_{ij}(\omega) = \psi_{ij}\hat{H}_i(\omega)\hat{H}_j^*(\omega), \tag{12}$$

where ψ_{ij} is the Fourier transform of the correlation between $m_i(t)$ and $m_j(t)$, and the asterisk indicates complex conjugate. Equation (12), in conjunction with (10) and (7), permits calculation of the noise on a string of repeaters from measurements on individual repeaters. Telephone repeaters are built the same for ease of manufacture. In the ideal case, $H_i(\omega) = H(\omega)$ for all values of i; furthermore, $\psi_{ij} = \psi_c$ for all $i \neq j$, and $\psi_{ii} = \psi_s$, for all i values of j. Equation (12) reduces to

$$\begin{aligned} \mu_{ij}(\omega) &= \psi_c(\omega)H^{N-i}(\omega)[H^{N-1}(\omega)]^* \qquad i \neq j \\ &= \psi_s(\omega)|H|^{2(N-i)} \qquad i = j. \end{aligned} \tag{13}$$

Equation (7) becomes

$$p_n = \int_{-\infty}^{\infty} |G(\omega)|^2 d\omega \left[\sum_{i=1}^{N} \psi_s |H|^{2(N-i)} + 2 \sum_{i=1}^{N-1} \sum_{j=i+1}^{N} \psi_c H^{N-i}(\omega)H^{N-j}(\omega)^* \right]. \tag{14}$$

A.3 Law of addition

In systems calculations, it is common to make the simplifying assumptions that the intermodulation power from all repeaters is the same and that the correlation of the intermodulation is the same between any two repeaters. Neither assumption is true, but since a large number of repeaters is involved, average quantities may be used if the distributions of noise and correlation are narrow. If, in this case, the total intermodulation power in a narrow band over a tandem connection of repeaters N is P_N in dBm, and the intermodulation power of any one repeater in the same narrow band is P in dBm, then the law of addition, Δ, is defined as

$$P_N = P + \Delta \log_{10} N. \tag{15}$$

The value of Δ is 10 for incoherent (power) addition and 20 for coherent (voltage) addition. The advantage of using the law of addition is that $\Delta \log_{10} N$ and the required NPR for a third-order dominated system both enter the system noise equations as the sum, $\Delta \log_{10} N$ + NPR. Therefore, for the same noise performance, the NPR must improve by the same amount that $\Delta \log_{10} N$ grows larger.

To relate Δ to the correlation of the intermodulation noise between any two repeaters, assume that $H(\omega) = 1$, so that

$$\rho = M_{ij}(0)/M_{ii}(0) \tag{16}$$

and

$$p = M_{ii}(0), \tag{17}$$

where $10 \log p = P$. Then eq. (7) becomes

$$p_N = Np[1 + (N - 1)\rho]. \tag{18}$$

The definition of eq. (15) gives

$$\Delta = 10 \left\{1 + \frac{\log_{10}[1 + (N - 1)\rho]}{\log_{10} N}\right\}. \tag{19}$$

Whereas ρ is a constant for any length system, Δ depends on N. Notice that, for $\rho \neq 0$, $\Delta \to 20$ for $N \to \infty$. In any case, $\rho = 0$ corresponds to $\Delta = 10$, and $\rho = 1$ to $\Delta = 20$, as would be expected.

APPENDIX B

Errors in Noise Loading Measurements

Errors in a measurement of intermodulation power were given in Section II and are reviewed here. In addition, errors in correlation measurements are given.

B.1 Intermodulation power and NPR

In Section II, the basic error in an intermodulation power measurement with this set was given as ± 0.25 dB, or 0.14 dB 1 σ. All errors are independent, so that error bars on Fig. 10 for assumed power or voltage addition are derived by summing the variances of the errors for each repeater measurement.

B.2 Errors in estimates of correlation coefficient

The correlation coefficient is defined as

$$\rho_{ij} = \frac{M_{ij}(0)}{\sqrt{M_{ii}(0)M_{jj}(0)}}. \tag{20}$$

Amplitude errors occur in the measurement of intermodulation, but these do not affect the correlation. The significant sources of error are extraneous delays between the two signals being measured and sample size. Extraneous delays are delays introduced by the measurement equipment, rather than true signal delays in the repeatered string under test. In heterodyne single-sideband repeaters, such extraneous delay may

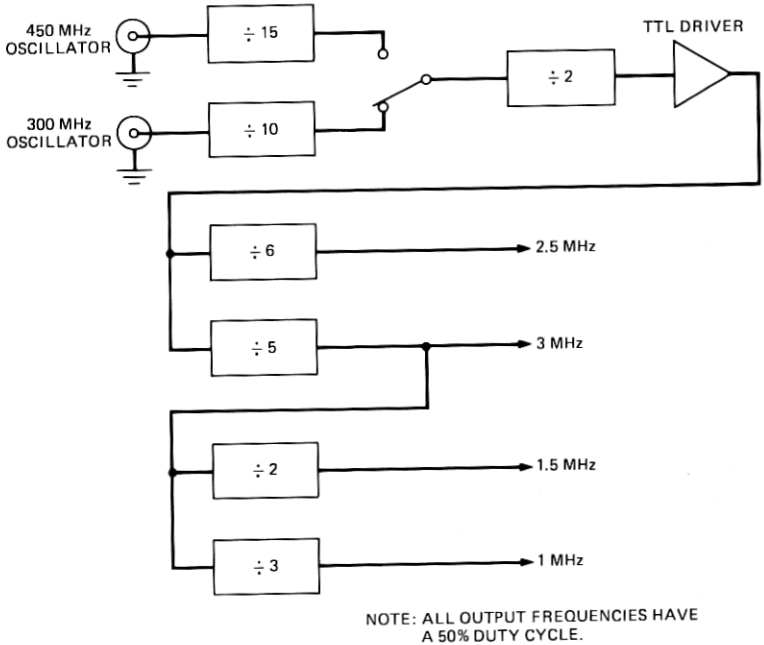

Fig. 12—Digital oscillator divider chain.

come from improperly functioning phase-locked loops. The error due to these delays in our data was estimated to have a standard deviation of 3 percent of the computed correlation.

The error in the correlation coefficient due to sample size may be estimated by assuming that the intermodulation noise in a notch is gaussian. For the noise-loading set used, the line spacing was about 200 Hz with a notch width of nearly 3 kHz, giving 15 lines for an intermodulation signal. This number of sine waves is well approximated by gaussian statistics.[5] The approximate mean and variance of an estimate of the correlation coefficient is $(\frac{1}{2})\log(1 + \rho/1 - \rho)$ and $1/(n - 3)$, respectively, where n is the number of points, and ρ is the estimate.[6] For the 255 data points available from the averager, this comes to a standard deviation of the error of about 6 percent. The standard deviation of the total error in an estimate of correlation is about 7 percent.

APPENDIX C

6-GHz Noise Loading Set

In the latter part of 1974 and early 1975, another PRNL set was designed for the 6-GHz band. Besides a much improved physical design, this set was designed with all LOs derived from a single source. This change reduced the cost of LO generation and also simplified the master

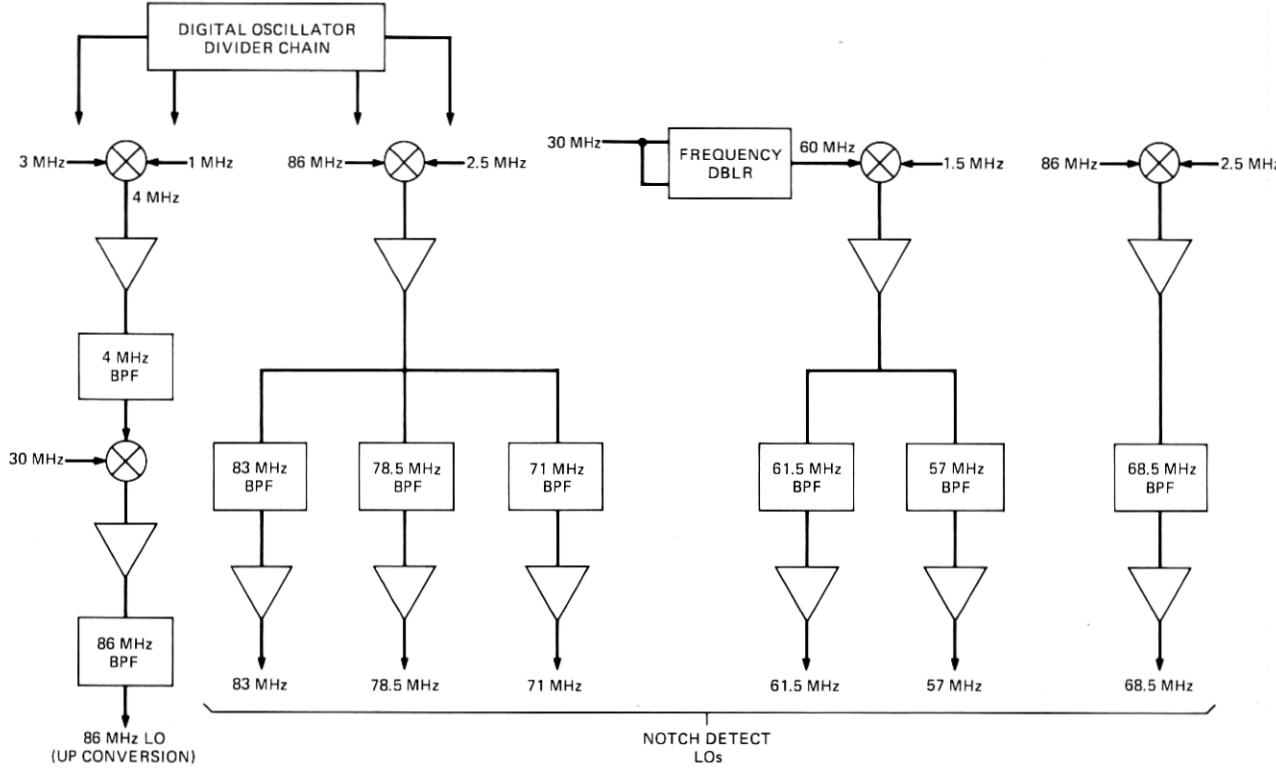

Fig. 13—Local oscillator frequency generation.

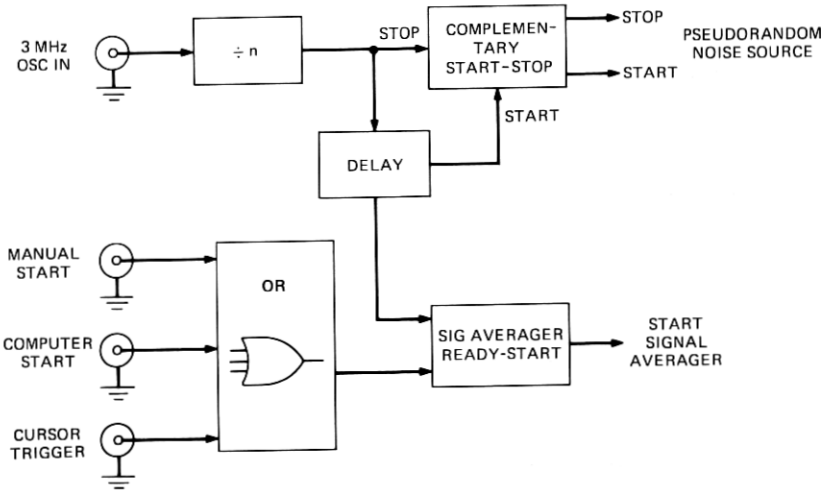

Fig. 14—Master timing circuit.

timing circuit. In addition, the set was designed to operate in the 4-GHz band with minimal changes. These design changes are described below.

In the 6-GHz set, only one master oscillator is used, either 300 MHz or 450 MHz (see Fig. 12), depending on whether a 20-MHz or 30-MHz IF is desired.

Using digital dividers, a number of basic frequencies are derived from this single oscillator. Double balanced mixers (see Fig. 13) are used to combine the appropriate basic frequencies as well as notch-detector frequencies. Crystal filters select the local oscillators so that spurs are more than 70 dB down. This keeps signal leakage into the notches at tolerable levels.

The block diagram for the new master timing circuit is shown in Fig. 14. The major difference between this and the previous circuit is the absence of the coincidence circuit. This circuit could be eliminated since all local oscillator frequencies, as well as all notch-select frequencies, are derived directly from one master oscillator. If the pseudorandom source repetition frequency is made a multiple of the lowest common denominator for all these LOs, coherence is assured. This lowest common denominator is 0.5 MHz, and the source frequency is usually chosen as 192.3 Hz, i.e., 2600 periods of the 0.5 MHz frequency.

Each single cycle of the test signal has to be slightly larger than the 5.12-ms single-sweep average period. This is achieved by setting the divide-by-n counter to the desired period. The complementary start-stop circuit, the delay circuit to assure a minimum reset period, the combining of Start commands (manual start, computer start, cursor trigger),

and the ready circuit are all similar to those shown in Fig. 3. The principal difference is simply the absence of the coincidence circuit. The strobe circuit is not needed since all notch-detect frequencies are coherently related to the 3-MHz oscillator frequency used to set the source period.

Output pulse jitter for this circuit is less than 0.25 ns, which makes it possible to achieve 42-dB signal-to-noise improvement routinely.

REFERENCES

1. *Transmission Systems for Communication,* Fourth Edition, Bell Laboratories, Inc., 1970.
2. P. O. Roberts, and R. H. Davis, "Statistical Properties of Smoothed Maximal-length Linear Binary Sequences," Proc. IEE, *113,* No. 1 (January 1966), pp. 190–196. See also additions by I. G. Cumming, "Autocorrelation Function and Spectrum of a Filtered, Pseudorandom Binary Sequence," Proc. IEE, *114,* No. 9 (September 1967), pp 1360–1364.
3. K. Y. Chang, "Intermodulation Noise and Products Due to Frequency-Dependent Nonlinearities in CATV Systems," IEEE Trans. Commun., *COM-23,* No. 1 (January 1975), pp. 142–155. Unpublished studies by C. D. Anderson, J. W. Smith, and L. L. Sheets of Bell Laboratories.
4. Y. W. Lee, *Statistical Theory of Communication,* New York: John Wiley, 1960, Chapter 13.
5. M. Slack, "The Probability Distributions of Sinusoidal Oscillations Combined in Random Phase," IEE Journal, *93,* Part III (March 1946), pp. 76–86.
6. K. A. Brownlee, *Statistical Theory and Methodology in Science and Engineering,* New York: John Wiley, 1961, p. 365.